

Research

Comparison of potential evapotranspiration methods in Ethiopia

Antensay Mekoya¹ · Mulatu Workneh²

Received: 30 December 2023 / Accepted: 21 March 2024

Published online: 09 April 2024

© The Author(s) 2024 [OPEN](#)

Abstract

The Food and Agricultural Organization method for estimating reference crop evapotranspiration (ET_o), FAO56, is the standard method across the globe. Daily ET_o estimated using seventeen potential evapotranspiration (PET) methods that has less data requirements were compared with FAO56 at five sites in Ethiopia (Bahir Dar, Bale Robe, Hawassa, Metehara, and Nazareth). The average rank of five model validation metrics namely standard deviation, RMSE, MAPE, NSE, and correlation were used to compare the methods. By taking the areal average ET_o and PET, ten methods, Wen, Ant, Pen, Mak, PT, Ha5, Ha4, Tho, Rad, and Enk, having correlation > 0.57 and MAPE $< 28\%$ were ranked 1st to 10th, respectively. Also, at each site, the above ten PET methods were compared. By taking the average ranks of the five sites, Wen, Pen, Ant, PT, and Mak & Ha5 ranked 1st to 5th, respectively. Wen & Ant methods which are applied in Ethiopia for the first time had shown the best performance.

Keywords Daily evapotranspiration · PET models · Tropical climate · Model validation metrics

1 Introduction

Evapotranspiration (ET) is the simultaneous process of water loss from the soil surface by evaporation and from the crop by transpiration [1]. It consists of evaporation from open water, bare soil, and rainfall interception as well as transpiration from plants [2]. Evapotranspiration (ET) is a key process in the energy and hydrologic budget of the earth with implications in water management works such as agriculture and hydropower generation. For irrigation planning, ET is a prerequisite [3]. Accurate quantification of ET, especially in arid or semiarid areas, is important in agroecosystems management to efficiently use water resources such as in irrigation management, water allocation, environmental assessment, protecting ground and surface water quality, and evaluating water yield for changing land use [4].

ET has also an important role in the land surface energy and hydrologic cycles [2]. On average, across all continents, the annual ET amount is about 70% of annual precipitation. This figure varies from up to 90% in dry regions (e.g., Australia) to approximately 60% in Europe [5]. Changes in actual evapotranspiration (AET) will change atmospheric dynamics which have a direct impact on weather and climate as it changes the sensible and latent heat energy partitioning [6]. Thus, the global water cycle and energy budget and their role in the climate system can be understood by a detailed understanding and knowledge of changes in regional and global ET [7].

Actual evapotranspiration (AET) is measured by lysimeter, Bowed ratio, or the eddy covariance technique [8]. In contrast to routine meteorological observations, in many regions across the world, in-situ measurements of AET are not

✉ Antensay Mekoya, antensaymekoya@yahoo.com | ¹Ethiopian Forestry Development (EFD), Ethiopia Environment and Forest Research Institute (EEFRI), Bahir Dar, Ethiopia. ²Ethiopia Meteorology Institute (EMI), National Meteorology Agency of Ethiopia (NMA), Bale Robe, Ethiopia.



available [9]. Evapotranspiration is a complex and nonlinear phenomenon because it depends on several interacting climatological factors such as temperature, humidity, wind speed, radiation, type and growth stage of a crop [10, 11]. Since direct measurement of AET using lysimeter measurement is a difficult task, potential evapotranspiration (PET) and Class A pan evaporation measurements have been used to estimate AET [12, 13]. PET is usually estimated using empirical methods or equations or PET models and cannot be directly observed [14]. PET denotes the upper limit of AET and it is used to estimate AET [9]. Note that PET is the total possible amount of moisture evaporating from the land surface that would occur with sufficient water supply and under certain meteorological conditions without advection and heating effects whereas AET is the total amount of ET that occurs [13, 15, 16].

Nowadays, PET and reference evapotranspiration (ET_0) are considered to be the same [17]. The Penman–Monteith method of the Food and Agricultural Organization (FAO56) of estimation of reference crop evapotranspiration or simply reference evapotranspiration denoted by ET_0 is the ET rate from a reference surface, not short of water [1]. This method was developed for a reference hypothetical crop with an assumed 0.12 m height, 70 s m^{-1} surface resistance, and albedo = 0.23, resembling closely actively growing and adequately watered green grass of uniform height and the evaporation from its extensive surface, [1]. The equation by [1] has been suggested as the standardized ET_0 equation, but it has a high climatic data requirement. As a result, there is a practical need to find other best alternative methods to estimate ET_0 in the areas where full climatic data are deficient [18]. From the available conventional methods, selecting the most reliable methods requires selecting methods that give reliable results with preferably minimum data prerequisite [19]. Moreover, the methods result in different estimates due to different data requirements, the different climate regions, etc. they are based on. That means ET varies according to weather and climate conditions. Hence, for a particular climate region, the most reliable method(s) has to be identified and selected from the available numerous methods or a new method that is suitable for that particular climate condition has to be developed. In this regard, many studies have been conducted to compare the different PET models [3, 16, 20, 25]. The studies concluded quite differently and PET models vary across climate regimes. Thus, Numerous PET formulae exist.

Based on the types of input variables [25], and [26] classified PET models into three groups namely radiation-based, temperature-based, and combination models. PET models can also be classified into five main groups: (1) water budget, (2) mass transfer, (3) radiation-based, (4) temperature-based, and (5) combinational [27]. For example, the Penman–Monteith (FAO56) method of estimation of reference crop evapotranspiration which is widely used for estimation of PET is one of the combination models.

A few studies in Ethiopia have evaluated the performance of PET models using either a short period observations [28, 29] or a single station [30]. Their result may not be representative of the climatology (a long period average) and for a large area like Ethiopia where the climate varies regionally. Thus, evaluating the performance of different PET models over longer periods in different areas across Ethiopia with different climate regimes was a necessity [20]. In this study, for the period 1982–2020, the performance of seventeen PET models in five climatologically different sites across Ethiopia is evaluated with reference to the ET_0 estimated using the FAO56 (Penman–Monteith) method.

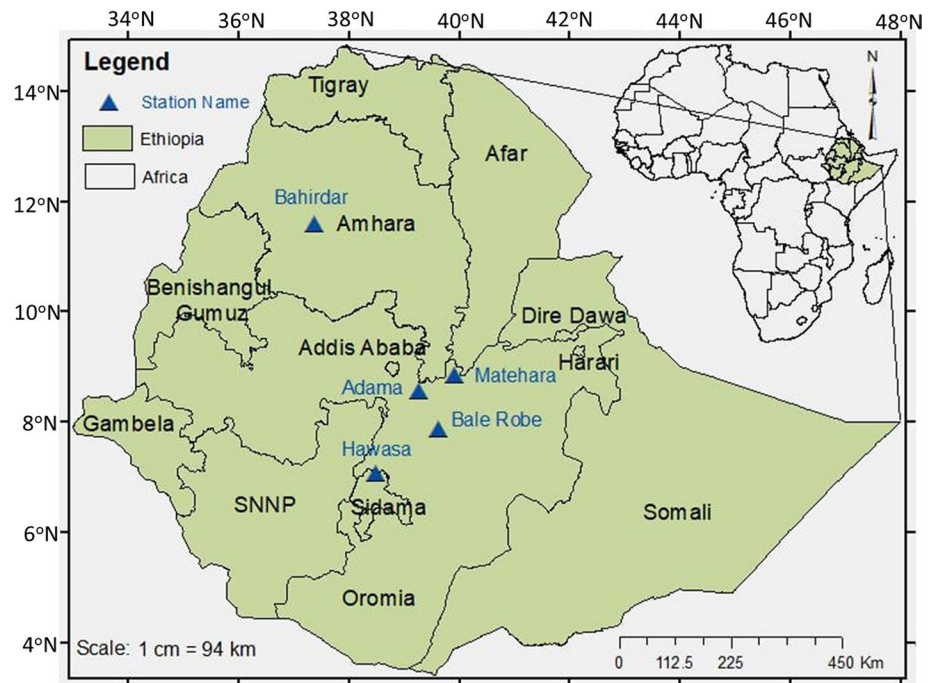
Therefore, the merit of this study is to identify the most reliable method that can be used for estimation of ET_0 or PET in places which lack full meteorological data to estimate ET_0 using [1] (FAO56). Thus, the finding of the study is more relevant for countries having less number of synoptic or principal meteorological stations such as Ethiopia. Ethiopia is selected as a case study because the number of stations recording meteorological parameters that are necessary for calculating ET_0 are limited in number and they are sparsely distributed. Also, most of the stations have shorter records (observation time) with missing values.

2 Materials and methods

2.1 Study area

The study was conducted at five sites in Ethiopia (Fig. 1). Ethiopia is located in the Horn of Africa. The climate in Ethiopia varies from dry to sub-humid [31]. Ethiopia's climate is multifaceted in the interior short horizontal distances; climates from tropical to sub-humid and subtropical to arctic can happen [32]. 43% of Ethiopia is highland (altitude above 1500 m a.s.l.) covering the whole 72 zones of Ethiopia [33]. Almost half of all the highlands of Africa are found in Ethiopia [30]. The major rain season for the highlands of Ethiopia is between June and September [34]. In Ethiopia, the summer period, June–September, is locally known as 'Kiremt'; Kiremt is the rainy period representing 50–70% of the mean annual rainfall. The winter period, October–January, is locally known as 'Bega'; Bega is the dry season in most parts of Ethiopia except

Fig. 1 Study area, Ethiopia located in East Africa, and five Meteorological stations



some southern parts. February-May is locally known as 'Belg'; Belg is the second rainy period in most parts of Ethiopia representing 20–30% of the mean annual rainfall.

For the five study sites namely Bahir Dar, Bale Robe, Hawassa, Metehara, and Nazareth (Adama) cities, climate data was obtained from the Ethiopia Meteorology Institute formerly called the National Meteorology Agency of Ethiopia (NMA), and its regional offices at Bahir Dar, Bale Robe, Hawassa, and Nazareth. Bahir Dar city which is one of the most beautiful cities in Africa is the capital of the Amhara regional state of Ethiopia where 85% of the water of the longest river in the World (the Nile River) originates. The Nile flows within the city of Bahir Dar. Also, the largest lake in Ethiopia, Lake Tana (area: 2156 km²), is also part of the city. Currently, the Amhara region is characterized by erratic rainfall, high land degradation, high population density, high rate of poverty and malnutrition [35] and it has a monsoonal climate with annual rainfall varying between 800 and 3000 mm and annual evapotranspiration amid 1400 and 1681 mm [30]. Bale Robe is the capital town of the Bale zone or district; 10 years ago Bale Goba, which has more tourist attractions, was the capital city of the Bale district. Bale zone is characterized by bimodal rainfall categories with a total rainfall of about 590 mm in Kiremt, 560 mm in Belg, and almost no rainfall in Bega seasons. Bale is highly productive and suitable for agricultural activities. The highest elevations in Bale Highlands are at Mount Tcludimtu (4377 m) and Batu (4307 m). Hawassa, like Bahir Dar, is one of the most beautiful cities in Africa. It is the capital city of the southern part of Ethiopia. Lake Langano (area: 230 km²) is in the vicinity of Hawassa. Hawassa, Metehara, and Nazareth cities lie in the great rift valley of Africa. Metehara station is characterized by an arid and semi-arid environment. In the district surrounding Metehara & Nazareth cities, livestock production is the main source of income for the communities followed by mixed crop livestock production [36].

2.2 Data

For the years from 1982 to 2020, 14,245 observations for each daily meteorological parameter such as precipitation (P), maximum air temperature (T_{max}), minimum air temperature (T_{min}), air Temperature (T), relative air humidity (RH), wind speed at 2 m (u_2), and sunshine hours/duration (SD) were obtained from Ethiopia Meteorology Institute (EMI). The percentage of missing data was above 0.8% for RH, u_2 , and SD while P, T_{max} , and T_{min} data have almost no missing values. The missing values for the three daily meteorological parameters (RH, u_2 , and SD) were filled fitting simple linear regression equation between observation data and global re-analysis data sets such as the National Aeronautics and Space Administration (NASA) and Climate Research Unit (CRU) data sets (Table 1).

Table 1 Brief overview of Meteorological Stations used in this study from 1982 to 2020. (

Station Name	Lat [°N]	Lon [°E]	Alt [m]	Mean, minimum, and maximum daily T [°C]	Minimum T _{min} and Maximum T _{max} [°C]	Mean, minimum, and maximum annual total rainfall [mm]
Bahir Dar	11.595	37.380	1800	19.5, 13.1, 27.2	0.0, 38.5	1330, 894, 1928
Bale Robe	7.875	39.622	2441	15.3, 7.5, 20.7	− 5.7, 31.9	765, 527, 991
Hawassa	7.065	38.483	1694	18.4, 10.3, 35.8	− 3, 44.9	1005, 638, 1278
Metehara	8.858	39.919	944	25.6, 12.2, 34.7	1.9, 41.5	520, 272, 770
Nazareth	8.55	39.283	1622	21.5, 10.6, 28.2	− 5.4, 37.6	862, 497, 1229

Lat = latitude, Lon = longitude, T = air Temperature, T_{max} = maximum air Temperature, T_{min} = minimum air Temperature)

2.3 Potential evapotranspiration (PET) models

The Food and Agricultural Organization (FAO) Penman–Monteith method (FAO56) for estimation of the reference evapotranspiration (ET_o) by [1] is taken as the sole standard reference method for estimating reference evapotranspiration as well as for comparing potential evapotranspiration across the world [37]. In this study, seventeen methods of estimation of potential evapotranspiration (PET) are compared with FAO56 method (see Eq. 2.7 in Table 2). The seventeen PET methods are selected based on literature review. For example, Enku (Enk) and Priestley Tayler (PT) are selected based on their particular suitability for the climate condition of Ethiopia (refer Table 2 for references). Penman (1963) (Pen) and Thornthwaites (1948) (Tho) are chosen because of their high global acceptance. Hargreaves's (1985) method (Har) which requires air temperature and extraterrestrial solar radiation which is computed from the latitude of the study site has been used in many countries. Wendling (1991) (Wen) is principally selected for data sparse areas. Antensay Mekoya's method (Ant) is recent and was applied to the climate of Germany; in this study, the suitability of this method for the climate of Ethiopia is checked. The Albrecht (Alb), Schendel (Sch), Turc (Tur), Makkink (Mak), and Blaney–Criddle (BC) methods are selected because they are applied in many tropical regions across the world. In a recent study by [20], the Hamon version2 temperature-based method (Ha2) is found to be the second best method next to FAO56 in estimating pan evaporation in China [20]. As compared to solar radiation, the effect of humidity and wind speed in estimating ET is relatively minimal [38–40]. Thus, the so-called solar radiation method (Rad) is also compared in this study. As compared to FAO56 (FAO), all seventeen methods are easy to apply and applied in many countries when a full set of climate data is not available.

2.4 Model validation metrics

The above seventeen PET models are compared with each other and with the reference method (FAO56) using model validation metrics such as Nash–Sutcliffe efficiency (NSE), root mean square error (RMSE), mean percent of error (MPE) or equivalently mean absolute percent of error (MAPE), standard deviation (s) or equivalently the standard deviation difference from the reference method (sd), and correlation (r) [20, 51–56]. The model evaluation statistics were applied by considering the reference method (FAO56) as measured (observed) values (x) while the rest seventeen PET models were taken as estimated (simulated) values (y). In the linear regression equation ('y = ax + b'), the y-intercept (b) and slope (a) indicate how well 'y' relates or matches with 'x'. The y-intercept indicates the presence of a lead or lag, or that the data sets are not perfectly aligned while the slope indicates the degree or magnitude of the relationship between model predictions and measured data[57].

2.5 Standard deviation (s)

$$s = \sigma = \sqrt{\frac{\sum (xi - \mu)^2}{N}} \quad (2.19)$$

Table 2 The PET models (methods) used in the study; for names of input variables see Table 3

Models or Methods of Estimation of PET	References	Eq
$PETPen = \left(\frac{\Delta}{\Delta + \gamma} (R_n - G) + kw * \frac{\gamma}{\Delta + \gamma} (aw + bw * u_2)(e_s - e_a) \right) / \lambda$	[37]	2.1
$PETWen = g * \left(\frac{G}{410} + (0.5 + 0.54 + u_2) * (100 - RH) * \frac{N}{905} \right)$	[41, 42]	2.2
$PETPT = \alpha \left(\frac{\Delta}{\gamma + \Delta} \right) (R_n - G) / \lambda$	[28]	2.3
$PETEnk = \frac{(T_{max})^n}{k}$	[29]	2.4
$PETAnt = (0.372R_s + 0.1312T_{max} - 0.028RH_{min} + 1.4866) / 3.24$	[41]	2.5
$PETRad = \left(\frac{R_n}{\lambda} \right)$	[43]	2.6
$PETFAO = \frac{0.408\Delta R_n + \gamma \frac{900}{T + 273} u_2 (e_s - e_a)}{\Delta + \gamma(1 + 0.34u_2)}$	[1]	2.7
For RH < 50%	as cited in [44]	2.8
$PETT_{ur} = 0.013 \left(\frac{T_{mean}}{T_{mean} + 15} \right) (R_s * 23.8846 + 50) \left(1 + \frac{50 - RH}{70} \right)$		
For RH > 50%		
$PETT_{ur} = 0.013 \left(\frac{T_{mean}}{T_{mean} + 15} \right) (R_s * 23.8846 + 50)$		
$PETMak = 0.61 \frac{\Delta}{\gamma + \Delta} \frac{R_s}{\lambda} 0.12$	as cited in [45]	2.9
$PETBC = p(0.46T_{mean} + 8.128)$	as cited in [44]	2.10
$PETA_{lb} = (0.1005 + 0.297 * u_2)(e_s - e_a)$	as cited in [46]	2.11
$PETTho = \begin{cases} C(-415.85 + 32.24T_{ef} - 0.43T_{ef}^2); T_{ef} > 26^\circ C \\ 16C \left(\frac{10T_{ef}}{l} \right)^a; 0^\circ C < T_{ef} < 26^\circ C \\ 0; T_{ef} \leq 0^\circ C \end{cases}$	as cited in [47]	2.12
Where, $l = 6.75 \cdot 10^{-7} l^3 - 7.71 \cdot 10^{-5} l^2 + 1.7912 \cdot 10^{-2} l + 0.49239$		
$PETHar = 0.0023(T_{max} - T_{min})^{0.5} (T_{mean} - 17.8)R_a$	[48]	2.13
$PETSch = 16 \frac{T_a}{RH}$	[46]	2.14
$PETHa2 = \left(\frac{SD}{12} \right)^2 e^{\left(\frac{T_a}{16} \right)}$	[49]	2.15
$ETHa3 = \left(\frac{SD}{12} \right)^2 e^{\left(\frac{T}{16} \right)}$	[49]	2.16
$PETHa4 = \left[0.5 + \left(\frac{SD}{12} \right)^2 \right] e^{\left(\frac{T}{16} \right)}$	[49]	2.17
$PETHa5 = \left[0.5 + \left(\frac{SD}{5 + SD_{mean}} \right)^2 \right] e^{\left(\frac{T}{16} \right)}$	[49]	2.18

where; s: sample standard deviation, σ : population standard deviation, μ : the population mean, xi: each value from the population, N = 14,245 days from 1/1/1982 to 31/12/2020: the size of the population. In this study, the standard deviation difference (sd) was calculated by subtracting the standard deviation of the reference method from the standard deviation of the PET models.

2.6 Nash–Sutcliffe model efficiency coefficient (NSE)

$$NSE = 1 - \frac{\sum_{t=1}^n (X_t - Y_t)^2}{\sum_{t=1}^n (X_t - X_m)^2} \quad (2.20)$$

where Y_t : is PET by each of the seventeen PET models or methods at time t, X_t : is PET by FAO56 method (FAO) at time t, and X_m : is the mean of PET by FAO56 method; t ranges from t = 1 to t = 14,245.

2.7 Root mean square error (RMSE)

$$\text{RMSE} = \sqrt{\left(\frac{1}{n}\right) \sum_{i=1}^n (\text{Ep}_i - \text{Et}_i)^2} \quad (2.21)$$

whereas Ep_i is estimated PET values by the 17 PET Models, Et_i tested data from cross-validation (PET by FAO56 method) and n is the total number of simulated values. It was used as the standard statistical metric providing a relatively high weight to large errors.

2.8 Centered root mean square error (CRMSE)

$$\text{CRMSE} = \sqrt{\left(\frac{1}{n}\right) \sum_{i=1}^n [(\text{Ep}_i - \text{Ep}_{\text{mean}}) - (\text{Et}_i - \text{Et}_{\text{mean}})]^2} \quad (2.22)$$

CRMSE is centered as the mean values of the data (observations and predictions) are subtracted first.

2.9 Mean percentage of error (MPE)

$$\text{MPE} = \frac{1}{n} \sum_{i=1}^n \left(\frac{(Y_i - X_i)}{X_i} \times 100\% \right) \quad (2.23)$$

where $\text{MPE}=0$ is the optimal value and the positive and negative values of MPE indicate an over- and under-estimate of the PET estimates by the seventeen PET Models as compared to FAO56, respectively [58].

2.10 Mean absolute percentage of error (MAPE)

$$\text{MAPE} = \frac{1}{n} \sum_{i=1}^n \left(\frac{|Y_i - X_i|}{X_i} \times 100\% \right) \quad (2.24)$$

The mean absolute percentage error (MAPE) also called mean absolute percentage deviation (MAPD) is the most common measure used to know model (forecast) error; it works best if there are no zeros and no extremes to the data,

2.11 Correlation coefficient (r)

The correlation coefficient is an index of the degree of parallel relationship between observed and simulated data and Pearson's product-moment correlation coefficient (r) is calculated as shown below:

$$r = \frac{\sum_{i=1}^n (X_i - \bar{X})(Y_i - \bar{Y})}{\sqrt{\left[\sum_{i=1}^n (X_i - \bar{X})^2\right]} \sqrt{\sum_{i=1}^n (Y_i - \bar{Y})^2}} \quad (2.25)$$

where X_i is the i th observation for the constituent being evaluated, Y_i is the i th simulated value for the constituent being evaluated, n is the total number of observations, and the overbar denotes the mean for the entire period of the evaluation with r ranging from -1 to 1 . If $r=0$, no linear relationship exists. If $r=1$ or -1 , a perfect positive or negative linear relationship exists, respectively.

2.12 Methodology (research design)

This study compared and evaluated the performance of seventeen selected PET models in estimating reference evapotranspiration (ET_o) over five sites in Ethiopia (see Appendix 1). First, daily PET values were calculated for each of the five sites using the seventeen PET models. The Penman–Monteith (FAO56) method for estimating crop reference evapotranspiration (ET_o) simply denoted here as 'FAO' was the reference method. Second, areal average ET_o and PET (for the seventeen models) computed using the five sites were used as a proxy value for Ethiopia. For precise comparison

of the performance of the seventeen PET models with each other, five ranks were computed for each of five validation metrics (statistical measures) namely standard deviation difference (sd), RMSE, MPE, NSE, and correlation (r). Then, the rank of the average rank of the five ranks was taken as a final rank. Third, out of a total of seventeen PET models, ten more reliable models having 1st to 10th rank, $r \geq 0.58$, and $\text{MAPE} \leq 27.3\%$ were screened for the next analysis. Note that the absolute values of sd & MPE (not shown in (Tables 4, 5, 6, 7, 8, 9)) were used to rank the seventeen and ten PET models over Ethiopia and in the five sites, respectively. While ranking, equal weight was given to each of the five validation metrics. Box plots and Taylor diagrams were also used for visual comparison. Fourth, for each of the five sites, the screened ten PET models were also compared with each other using FAO56 as the reference method. Validation metrics were also applied to compare the ten PET models with each other in a similar way as described for the seventeen PET models.

3 Results and discussions

3.1 Results

3.1.1 Areal average ranks of PET models

For each of the five sites, the correlation test showed that the seventeen PET models were significant at a 95% confidence level indicating that all are appropriate methods for estimation of reference evapotranspiration or potential evapotranspiration; $df = n - 2 = 14,243$, $p\text{-value} < 0.05$. Six PET models namely Alb, BC, Ha2, Ha3, Har, and Sch highly under or over-estimated PET ($\text{MAPE} > 47\%$); they had also lower correlation (see Table 4 and Fig. 2). On the other hand, one PET model namely Tur had negative correlation although it had not highly over- or under- estimated PET ($\text{MAPE} = 12.24\%$). The average of the five sites ET_0 can be used as a proxy value for Ethiopia particularly in data-scarce areas. On the basis of the areal average of the five sites, Wen, Ant, Pen, Mak, PT, Ha5, Ha4, Tho, Rad, and Enk ranked 1st to 10th (see Table 4 and Fig. 2).

3.1.2 Rank of PET models over selected five sites in Ethiopia

For each of the five sites the ten PET models (Wen, Ant, Pen, PT, Mak, Ha5, Ha4, Tho, Rad, and Enk) which were ranked 1st to 10th, respectfully were selected for next steps (see Table 4 and Fig. 2). For a site, the rank of the average rank of the five statistical measures was used as a measure to compare the ten PET models. For example, at Bahir Dar site, as seen in Table 5, PT, Pen, Wen, Ant, and Ha5 were ranked 1st to 5th (see also Figs. 3, 4). At Bale Robe and Hawassa sites, PT and Tho got the first rank while Wen was ranked first at two sites, at Metehara and Nazareth sites (see (Tables 6, 7, 8, 9, Figs. 5, 6, 7, 8, 9, 10, 11, 12)).

3.2 Discussions

3.2.1 Areal average ranks of PET models

The NSE values were relatively ranged from -255.40 to 0.36 . The largest drawback of NSE was that calculation of squared values was required to show the relationships among the measured and the imitation values which may result in over- and under-estimation of larger values while the lower values were neglected [59, 60]. As suggested by [28] the Priestley-Taylor calibrated method as the most suitable method for ET estimation in Ethiopia. In his study, Seleshi used monthly data from 167 stations found in different climatic zones of Ethiopia for the period from 2011 to 2015 to compare PT with BC and Enk methods using FAO as the reference method. The result of this study is in agreement with Seleshi; however, it has the advantage of using long-year daily data and consideration of many methods. In another study conducted using the last 20 years' daily climate data of 27 sites in the Nile Basin of Ethiopia to compare four methods, the estimated PET ranged from 3.5 to 5.5 mm/day [61]. Their result does not contradict the current study result (1.73–5.74 mm/day). Using four statistical measures and daily climate data from 1985 to 2014 for Malaysia, a tropical country like Ethiopia, [62] compared 31 methods. In their study, they found PT to be the most reliable method. In another similar study conducted for the evaluation of eight ET estimation methods using 30 years of daily data in Iran, PT was also the most reliable method [63]. The result of the above studies is in agreement with the result of this current study.

3.2.2 Rank of PET models over selected five sites in Ethiopia

For the Bahir Dar site [61], suggested that ET_o ranged from 2.06 to 4.54 mm/day and had a standard deviation of 0.77 while in this study it was 1.64–7.71 mm/day and 0.54, respectively. The calibrated Priestley-Taylor model was found to be the most reliable ([13, 28]). In a similar study that uses average ranks of statistical measures (validation metrics) to compare PET models with FAO, Mak obtained the 7th rank [51]. However, in another study conducted ten years ago, the Mak method was the most suitable method followed by Tur and PT [47]. [30] compared eight PET models and Piche pan evaporation with 11 years of Class A pan measurements and found that Enk is the most reliable method next to FAO. However, in this study, Enk was the 10th most reliable method. For Bale Robe ET_o ranged from 1.48 to 4.47 mm/day with a mean of 2.81 mm/day. In another study, the range and mean values of PET for Bale Robe and its surrounding areas were overestimated (3.1 to 3.9 & 3.4 mm/day, respectively) based on information extracted from five meteorological stations' data from 1987 to 2017 [64].

For the Hawassa site and its surrounding Rift Valley areas of Ethiopia such as Ziway, the PET estimates are expected to be similar. [38] used remotely sensed data to estimate Lake Ziway evaporation due to the limited availability of observed meteorological data. Using NOAA's spectral data from 1994 to 1995, PET was estimated to range from 4.6 to 6.1 mm/day with a mean and standard deviation of 5.6 mm/day and 0.5, respectively [65]. [65] also overestimated ET_o as compared

Table 3 List of input variables used for the calculation of PET models

Input variable name (Value; Reference)	Symbols	Units
Latent heat of vaporization (2.45 [49])	λ	MJ kg ⁻¹
Potential Evapotranspiration	PET	mm d ⁻¹
Wind function coefficient (6.43; [49])	k_w	–
Wind function coefficient (1.0; [49])	a_w	–
Wind function coefficient (0.537; [49])	b_w	–
Maximum temperature	T_{max}	°C
Minimum temperature	T_{min}	°C
Air temperature; $T = (T_{max} + T_{min})/2$	T	°C
Mean air temperature; for n observation values: $T_a = \sum_{i=1}^n T_i$	T_a	°C
Wind speed at 2-m height	u_2	m/sec
Relative air humidity	RH	%
Net radiation	R_n	MJ m ⁻² d ⁻¹
Slope vapor curve	Δ	kPa /°C
Mean daily percentage of annual daytime	P	hr
Saturation vapor pressure	e_s	kPa
Actual vapor pressure	e_a	kPa
Daily extra-terrestrial solar radiation	R_a	MJ m ⁻² day ⁻¹
Psychrometric constant	Γ	kPa /°C
Solar or shortwave radiation	R_s	MJ m ⁻² d ⁻¹
Coefficient; wet and dry phase ($48 * T_{max} - 330$; [28])	K	–
Coefficient; dry phase ($73 * T_{max} - 1015$; [28])	K	–
Coefficient; rain phase ($38 * T_{max} - 63$; [28])	K	–
Day length (the daylight hour)	N	hr
Daily soil heat flux density	G	MJ m ⁻² d ⁻¹
Daily sum of global radiation	G	J cm ⁻²
Surface albedo (1.26; [9])	α	–
Local constant (2.5; [29])	n	–
Daily minimum relative air humidity	RH_{min}	%
Sunshine duration (Sunshine hours)	SD	hr
Mean sunshine duration hour	SD_{mean}	–
Function depends on air temperature	G	–
Thermal index (a function of monthly temperature; [50])	I	–
Euler's number (2.71828 18,284)	e	–

Table 4 Statistical summary and rank of ten PET models as compared to FAO over Ethiopia

	Max	Mean	Min	s	Sd	R1	NSE	R2	RMSE	R3	MPE	R4	r	R5	Average Rank	Rank
FAO	5.89	3.24	1.64	0.5	0		1		0		0		1			
Alb	2.55	0.46	0.03	0.21	-0.29	10	-255.4	17	2.8	16	-87	17	0.74	5	13	15
Ant	4.65	3.44	1.51	0.51	0.01	1	-0.06	6	0.5	2	7.8	3	0.74	5	3.4	2
BC	8.5	5.72	0.02	1.64	1.14	16	-2.68	12	2.9	17	75.8	16	0.5	13	14.8	17
Enk	8.13	4.11	1.09	0.98	0.48	14	-0.5	9	1.18	10	27.3	10	0.62	9	10.4	10
Ha2	3.43	1.74	0	0.75	0.25	9	-4.18	15	1.68	12	-47.1	12	0.33	16	12.8	14
Ha3	4.66	1.76	0	0.8	0.3	11	-3.4	13	1.62	11	-47.3	13	0.53	12	12	11
Ha4	7.87	3.57	1.29	0.92	0.42	13	0.08	4	0.88	8	8.7	5	0.63	8	7.6	7
Ha5	7.15	3.3	1.28	0.81	0.31	12	0.18	2	0.7	6	0.8	1	0.64	7	5.6	6
Har	7.23	4.84	1.64	0.59	0.09	4	-7.98	16	1.74	13	53	14	0.42	14	12.2	12
Mak	5.07	3.57	1.29	0.62	0.12	6	0.16	3	0.58	5	11.4	4	0.78	3	4.2	4
Pen	6.45	3.75	1.8	0.54	0.04	2	0.06	5	0.54	3	16.1	8	0.98	1	3.8	3
PT	4.99	3.13	1.67	0.46	-0.04	2	-0.7	10	0.56	4	-1.4	7	0.77	4	5.4	5
Rad	7.07	3.94	2.18	0.65	0.15	7	-1.22	11	1.02	9	25.8	11	0.58	11	9.8	9
Sch	17.88	5.46	2.94	1.34	0.84	15	-3.8	14	2.6	15	66.8	15	0.42	14	14.6	16
Tho	5.72	3.71	1.04	0.7	0.2	8	-0.4	8	0.8	7	15	9	0.59	10	8.4	8
Tur	5.16	2.76	0.03	1.74	1.24	17	-0.28	7	1.98	14	-10.3	6	-0.08	17	12.2	12
Wen	5.06	3.5	1.34	0.59	0.09	4	0.36	1	0.48	1	9	2	0.8	2	2	1

Table 5 Statistical summary and rank of ten PET models as compared to FAO56 (FAO) at Bahir Dar

	Max	Mean	Min	S	sd	R1	NSE	R2	RMSE	R3	MPE	R4	r	R5	Average Rank	Rank
FAO	7.71	2.97	1.64	0.54	0		1		0		0		1			
Ant	4.77	3.42	1.53	0.57	0.03	2	-0.4	8	0.66	4	16.9	4	0.62	7	5	4
Enk	9.3	4.06	1.31	0.92	0.38	9	-1.1	11	1.32	11	38.2	10	0.6	8	9.8	10
Ha4	7.18	3.37	1.31	0.97	0.43	10	0.18	4	0.88	9	13.8	3	0.59	10	7.2	8
Ha5	6.53	3.14	1.31	0.85	0.31	8	0.32	3	0.7	6	6.1	2	0.6	8	5.4	5
Mak	5.15	3.54	1.35	0.67	0.13	6	-0.3	7	0.76	8	20.3	7	0.7	6	6.8	7
Pen	8.78	3.5	1.71	0.59	0.05	3	0.14	5	0.55	3	18.3	6	0.97	2	3.8	2
PT	5.7	2.79	1.29	0.49	-0.1	4	0.56	2	0.33	2	-5.7	1	0.87	3	2.4	1
Rad	5.2	3.58	1.65	0.54	0	1	-0.8	9	0.72	7	22	8	0.76	4	5.8	6
Tho	6.63	3.83	0.98	0.84	0.3	7	-0.8	9	1.13	10	30.8	9	0.5	11	9.2	9
Wen	5.36	3.44	1.37	0.65	0.11	5	0	6	0.66	4	16.9	4	0.72	5	4.8	3

Table 6 Statistical Summary and Rank of ten PET models as compared to FAO56 (FAO) at Bale Robe

	Max	Mean	Min	S	sd	R1	NSE	R2	RMSE	R3	MPE	R4	r	R5	Average Rank	Rank
FAO	4.47	2.81	1.48	0.44	0		1		0		0		1			
Ant	4.43	3.15	1.34	0.58	0.13	5	0.32	4	0.48	5	12	4	0.81	5	4.6	4
Enk	6.3	3.37	1	0.68	0.23	8	-0.47	8	0.82	10	20.9	9	0.48	7	8.4	10
Ha4	4.95	2.57	1.03	0.7	0.26	9	-0.23	7	0.78	8	-7	2	0.23	10	7.2	6
Ha5	4.49	2.4	1.03	0.61	0.17	6	-0.64	9	0.78	8	-13.4	5	0.24	9	7.4	7
Mak	4.83	3.24	1.2	0.71	0.27	10	0.31	5	0.59	6	14.6	6	0.86	3	6	5
Pen	5.02	3.27	1.63	0.5	0.06	3	0.12	6	0.47	4	16.5	7	0.99	1	4.2	3
PT	4.5	2.73	1.48	0.43	-0.01	1	0.66	2	0.25	2	-2.7	1	0.85	4	2	1
Rad	5.15	3.61	2.16	0.49	0.05	2	-2.09	11	0.86	11	29.2	10	0.76	6	8	9
Tho	5.22	3.31	1.15	0.51	0.07	4	-0.98	10	0.72	7	19.3	8	0.41	8	7.4	7
Wen	4.59	3.08	1.2	0.65	0.21	7	0.55	3	0.44	3	8.8	3	0.87	2	3.6	2

Table 7 Statistical Summary and Rank of Ten PET Models as compared to *FAO56 (FAO)* at Hawassa

	Max	Mean	Min	S	sd	R1	NSE	R2	RMSE	R3	MPE	R4	r	R5	Average Rank	Rank
FAO	4.84	2.82	1.57	0.4	0		0		0		0		1			
Ant	4.63	3.22	1.31	0.6	0.2	4	0.16	6	0.55	4	13.8	4	0.78	3	4.2	3
Enk	7.97	3.75	0.93	1.27	0.86	10	-0.24	9	1.41	10	31.6	9	0.62	2	8	9
Ha4	8.52	2.93	1.1	0.93	0.53	8	0.47	4	0.68	8	2.2	2	0.78	3	5	4
Ha5	8.36	2.87	1.1	0.9	0.5	7	0.49	3	0.64	6	0.3	1	0.78	3	4	2
Mak	4.9	3.33	1.22	0.7	0.3	6	0.12	7	0.66	7	17.1	6	0.84	7	6.6	7
Pen	5.54	3.33	1.69	0.48	0.08	3	-0.17	8	0.52	3	17.9	7	0.97	10	6.2	6
PT	5.04	3.6	2.2	0.45	0.05	2	-2.32	10	0.82	9	28.3	8	0.81	6	7	8
Rad	13.98	4.96	3	1.25	0.84	9	-2.83	11	2.44	11	77.4	10	0.31	1	8.4	10
Tho	4.05	2.72	1.59	0.39	-0.02	1	0.7	2	0.21	2	-3.3	3	0.89	9	3.4	1
Wen	4.79	3.25	1.27	0.67	0.26	5	0.26	5	0.57	5	14.4	5	0.85	8	5.6	5

Table 8 Statistical Summary and Rank of Ten PET Models as compared to *FAO56 (FAO)* at Metehara

	Max	Mean	Min	S	sd	R1	NSE	R2	RMSE	R3	MPE	R4	r	R5	Average Rank	Rank
FAO	6.3	3.93	1.87	0.57	0		0		0		0		1			
Ant	4.78	3.87	1.95	0.34	-0.23	6	-0.79	8	0.45	4	-0.3	1	0.63	10	5.8	5
Enk	8.64	5.17	0.96	1.05	0.48	9	-0.93	9	1.46	11	31.7	10	0.7	8	9.4	10
Ha4	11.16	5.1	1.6	1.08	0.5	10	-0.68	7	1.39	10	29.7	9	0.74	5	8.2	8
Ha5	9.72	4.55	1.6	0.92	0.35	8	0.1	4	0.87	8	15.7	6	0.76	4	6	6
Mak	5.29	3.98	1.4	0.45	-0.12	4	0.09	5	0.43	3	2.2	2	0.68	9	4.6	4
Pen	6.52	4.49	2.12	0.56	-0.01	1	-0.01	6	0.56	6	14.6	5	0.99	2	4	2
PT	5.1	3.21	1.55	0.48	-0.09	2	-1.67	11	0.79	7	-18.1	7	0.83	3	6	6
Rad	5.96	3.74	2.07	0.48	-0.09	2	0.11	3	0.45	4	-4.2	4	0.71	7	4	2
Tho	6.5	5.03	0.66	0.88	0.31	7	-1.31	10	1.33	9	29	8	0.52	11	9	9
Wen	5.42	4.02	1.48	0.45	-0.12	4	0.21	2	0.4	2	3.2	3	0.73	6	3.4	1

Table 9 Statistical summary and rank of ten PET models as compared to *FAO56 (FAO)* at Nazareth

	Max	Mean	Min	S	sd	R1	NSE	R2	RMSE	R3	MPE	R4	r	R5	Average Rank	Rank
FAO	6.15	3.68	1.64	0.55	0		0		0		0		1			
Ant	4.65	3.54	1.44	0.45	-0.11	6	0.44	6	0.33	3	-3.3	4	0.84	3	4.4	3
Enk	8.43	4.21	1.26	0.96	0.41	10	0.16	9	0.88	11	14.2	10	0.68	8	9.6	10
Ha4	7.52	3.89	1.4	0.92	0.37	9	0.57	4	0.61	8	5	7	0.82	5	6.6	6
Ha5	6.66	3.53	1.38	0.78	0.23	7	0.63	3	0.47	5	-4.7	5	0.82	5	5	4
Mak	5.19	3.77	1.26	0.55	0	1	0.57	4	0.36	4	2.9	3	0.8	7	3.8	2
Pen	6.41	4.17	1.86	0.56	0.01	2	0.25	8	0.49	6	13.4	9	0.99	2	5.4	5
PT	4.61	3.32	1.83	0.46	-0.09	5	-0.84	11	0.63	9	-8.7	8	0.5	10	8.6	9
Rad	5.04	3.8	2.02	0.49	-0.07	4	-0.51	10	0.6	7	4.7	5	0.37	11	7.4	8
Tho	6.19	3.66	0.82	0.9	0.35	8	0.39	7	0.7	10	-0.7	1	0.63	9	7	7
Wen	5.15	3.73	1.37	0.54	-0.01	2	0.66	2	0.32	2	1.6	2	0.84	3	2.2	1

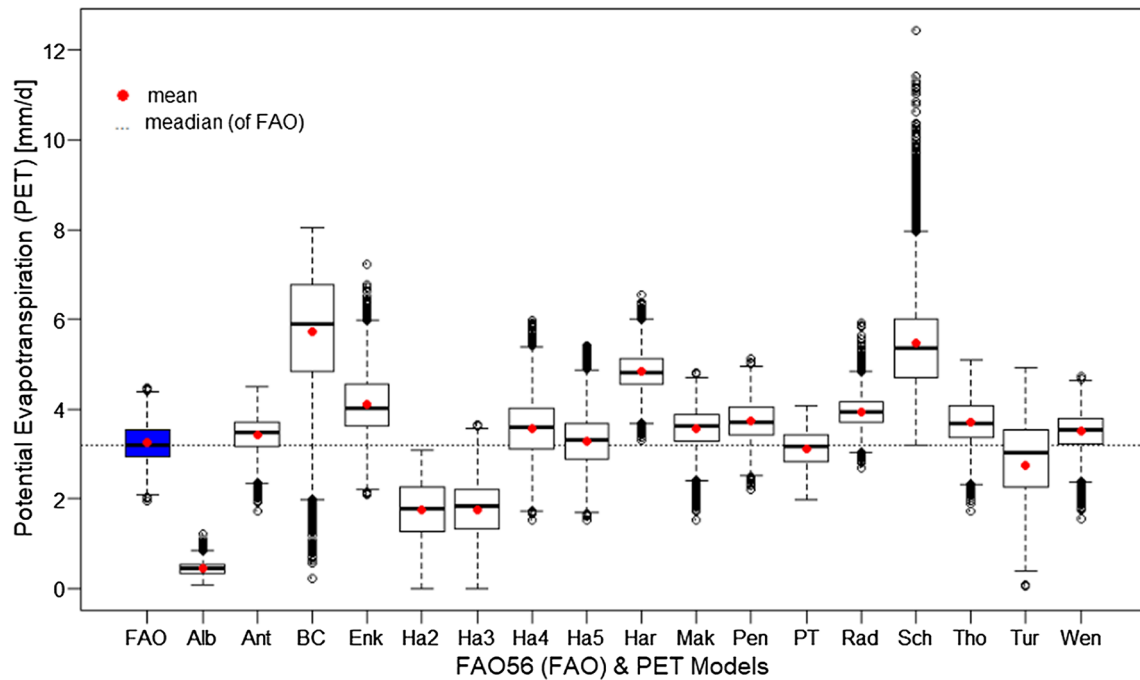
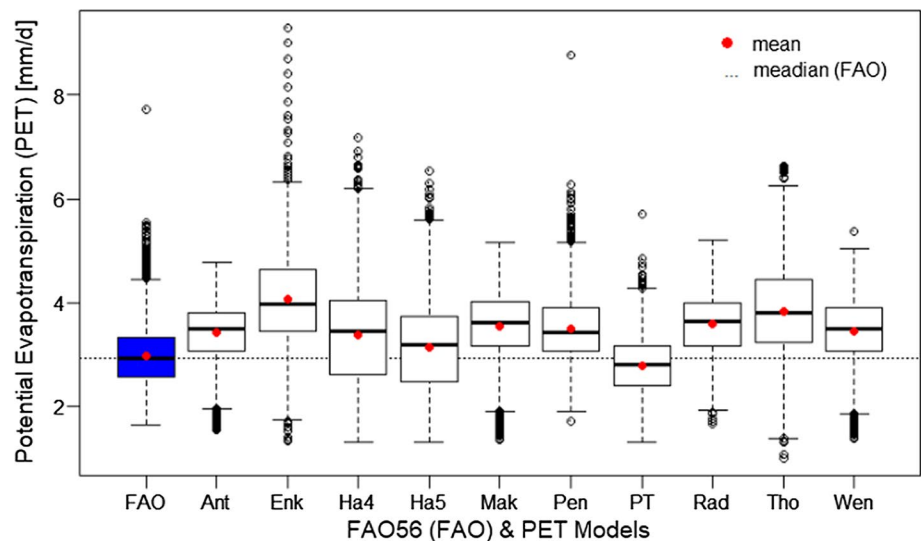


Fig. 2: 1982–2020 areal average FAO56 (FAO) and seventeen PET models (Alb to Wen) over Ethiopia

Fig. 3 Boxplot of the daily reference and potential evapotranspiration at Bahir Dar (1982–2020)



with the result of this study (range = 1.57–4.84 mm/day, mean = 2.82 mm/day, $s = 0.4$). In another similar study conducted in Malaysia to compare PET models using climate data from 1972 to 2001, Tho estimated ET_0 with the least error [47]. For the Metehara site and its surrounding areas, according to a study conducted in a similar climatic area with Metehara which is located in the Rift Valley of Ethiopia using climate data from 1977 to 2018, Tho was found to be the best method [66]. Nazareth (Adama) is also located in the Rift Valley of Ethiopia. For Nazareth and its surrounding areas, Wed & Mak were found to be the most reliable PET models. The result of this study (see (Tables 5, 6, 7, 8, 9) agrees with the findings of a study conducted using monthly average daily data from 1950 to 2014 [9]. In another study conducted in Tharandt, Germany using ten minutes and daily climate data from 2004 to 2014, Wen was found to be the most reliable method [67]. Mak method is preferred for a region where its geographic feature is multifaceted such as southern China where all the calculated values were based on daily (1962–2013) meteorological data [17].

Fig. 4 Taylor Diagram between FAO56 (FAO) and ten PET models at Bahir Dar (1982–2020)

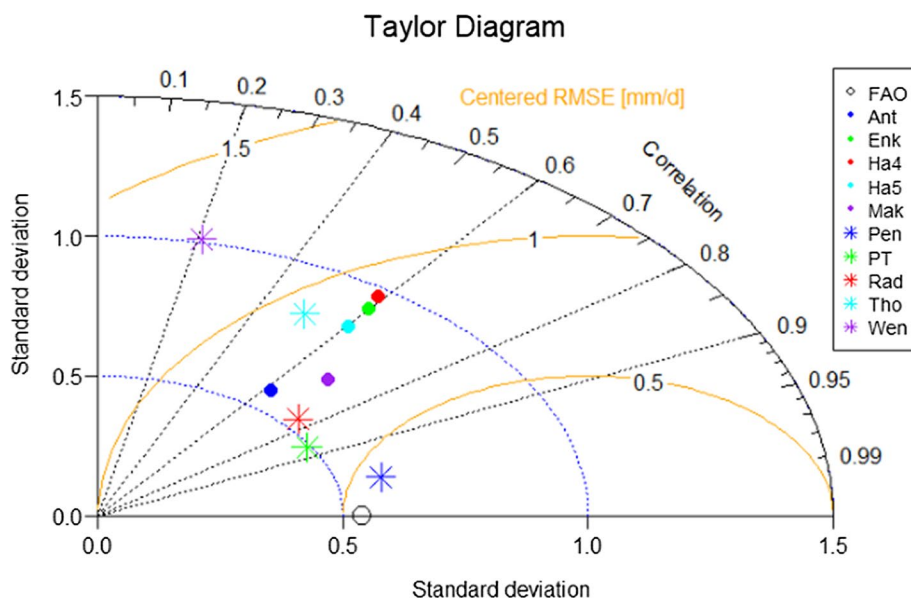
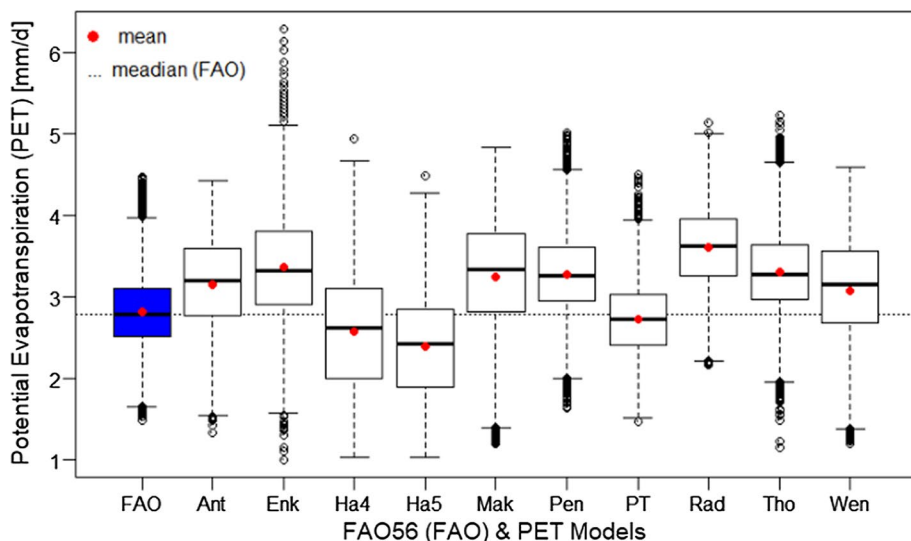


Fig. 5 Boxplot of the daily reference and potential evapotranspiration at Bale Robe (1982–2020)



3.2.3 Justification of the results

The best performed models for estimation of ET_o at the five sites in Ethiopia were Wen or PET_{Wen} (Eq. 2.2), Ant or PET_{Ant} (Eq. 2.5), and Pen or PET_{Pen} (Eq. 2.1). Wen and Ant are radiation-based methods while Pen is combination method. According to [26], combination and radiation-based models give more reliable PET estimates compared to the mass transfer- and temperature-based methods. From the three best performed models, Wen and Ant are better than Pen (or they are preferred to Pen) due to their low data requirements. The two radiation-based models (Wen and Ant) are a function of relative air humidity (RH). RH may have significant impact in PET or ET_o estimation in Ethiopia. It may also be a dominant meteorological parameter affecting ET_o changes in the country. Thus, the justification of the result may require further study.

Fig. 6 Taylor Diagram between FAO56 (FAO) and ten PET models at Bale Robe (1982–2020)

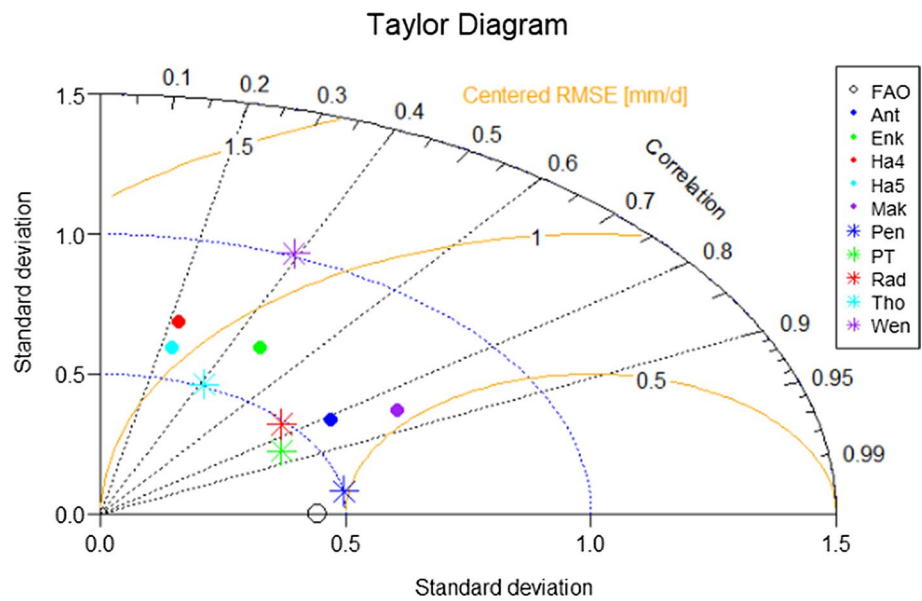
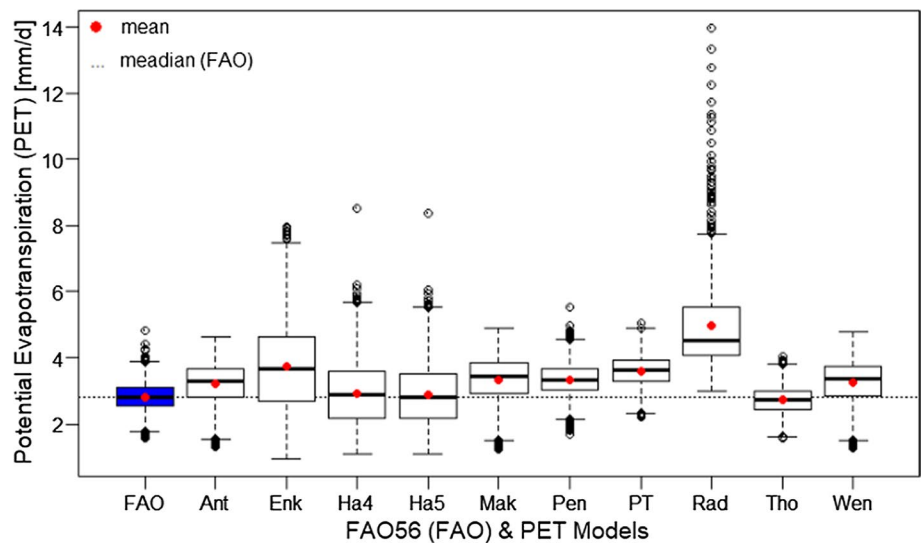


Fig. 7 Boxplot of the daily reference and potential evapotranspiration at Hawassa (1982–2020)



4 Summary, conclusions and recommendations

4.1 Summary

For five sites in Ethiopia namely Bahir Dar, Bale Robe, Hawassa, Metehara, and Nazareth daily potential evapotranspiration (PET) values were calculated for selected seventeen PET models using 39 years (1982–2020) of daily meteorological data such as maximum and minimum air temperature, maximum and minimum relative air humidity, wind speed at two meters above the ground, and sunshine duration hours. The Penman–Monteith (FAO56) method was used as the reference method to calculate daily reference evapotranspiration (ET_0) values. Then, in each site, the seventeen PET models’ daily values were compared with ET_0 values. Out of the seventeen PET models, ten PET models with correlation ≥ 0.58 and mean absolute percent error (MAPE) $\leq 27.3\%$ were selected (screened) as reliable methods for the estimation of ET_0 or PET in Ethiopia, particularly at the five sites. Wen, Ant, Pen, PT, Mak, Ha5, Ha4, Tho, Rad, and Enk, ranked first to tenth, were

Fig. 8 Taylor Diagram between FAO56 (FAO) and ten PET models at Hawassa (1982–2020)

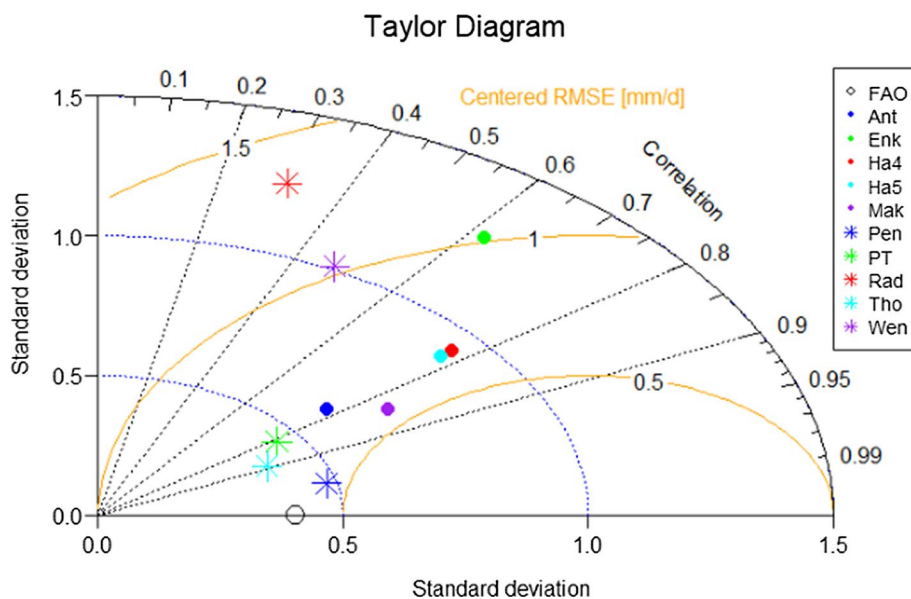
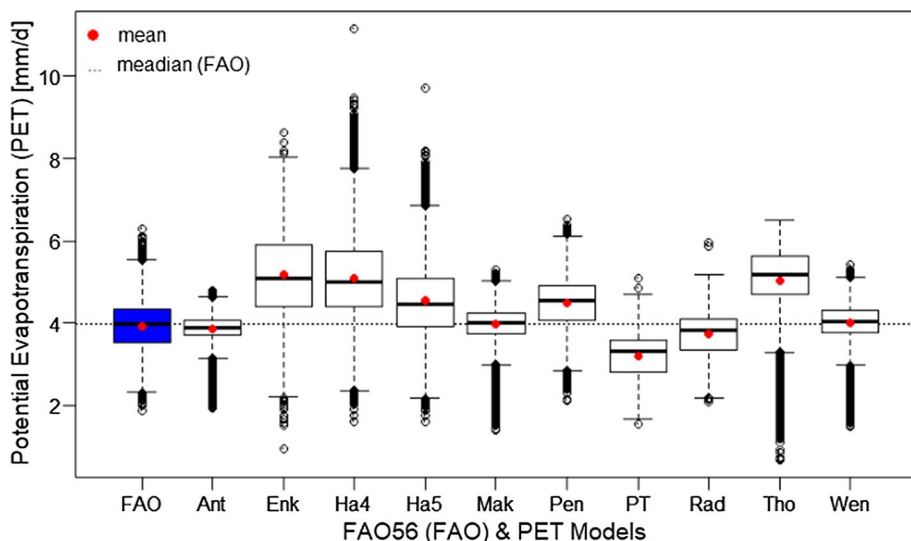


Fig. 9 Boxplot of the daily reference and potential evapotranspiration at Metehara (1982–2020)



taken as reliable PET models for estimating ET_o or PET over Ethiopia. To compare and rank the seventeen and ten PET models over Ethiopia and at the five sites, the rank of the average rank of five model validation metrics namely standard deviation (s) or equivalently standard deviation difference from the reference method, root mean square error (RMSE), mean absolute percent error (MAPE), Nash–Sutcliffe Efficiency (NSE), and correlation (r) were used.

The result showed that at Bahir Dar and Bale Robe sites and nearby areas Priestly-Taylor method (PT) was the best method while the Wendling method (Wen) was the best method for Metehara and Nazareth and in their vicinity. The method by Thornthwaites (Tho) was found to be the most reliable method for Hawassa and nearby areas. For each of the ten reliable PET models, by taking the average ranks of the five sites, Wen, Pen, Ant, PT, Mak, and Ha5 were found to be the most reliable methods in the five sites; ranked 1st to 6th, respectively.

International relevance (appeal statement) All the methods used in the study are standard methods of estimation of PET. The comparison is also performed using standard model validation metrics. Thus, the models used in this study are useful to compare and identify the most reliable methods of estimation of PET in a particular place across the world. The models can be used by practitioners following Table 2. For example, to estimate ET_o using the Wendling (1991) and

Fig. 10 Taylor Diagram between FAO56 (FAO) and ten PET models at Metehara (1982–2020)

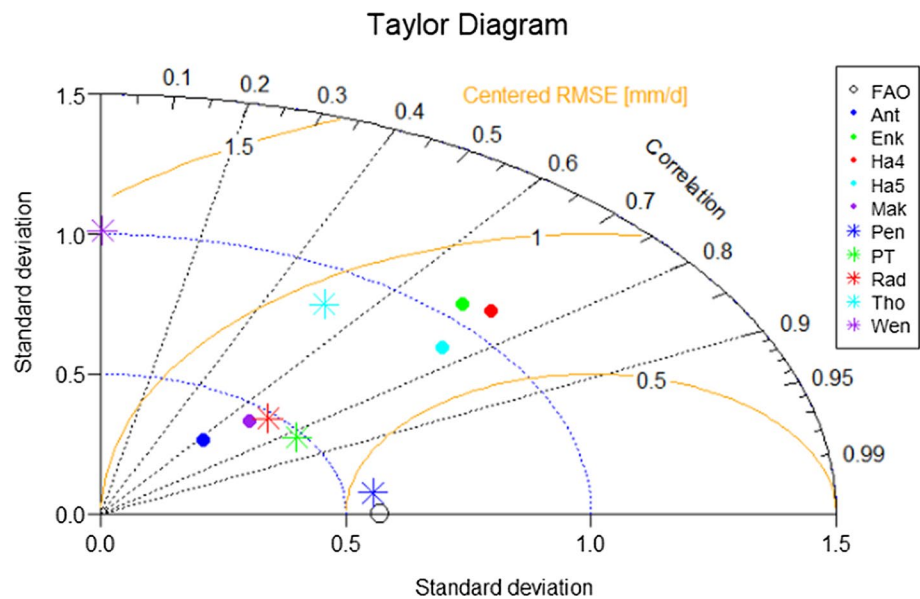
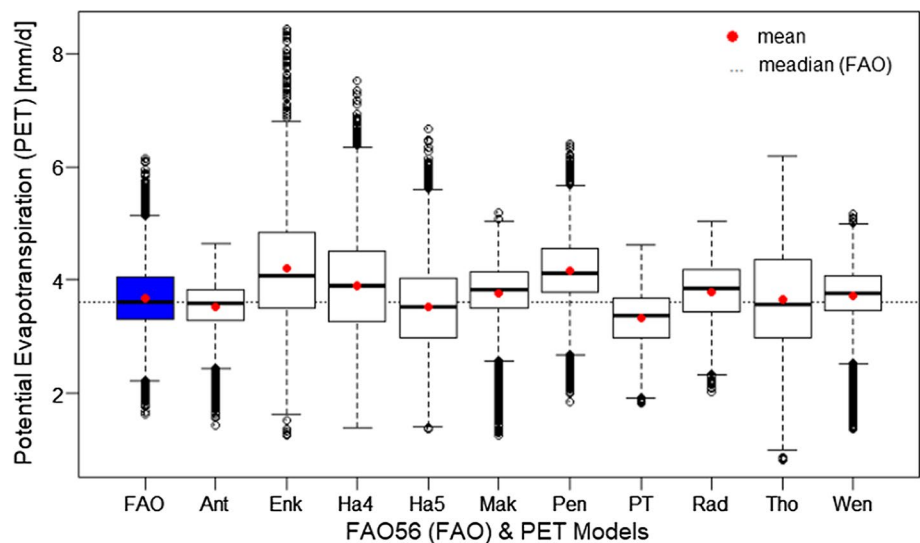


Fig. 11 Boxplot of the daily reference and potential evapotranspiration in Nazareth (1982–2020)

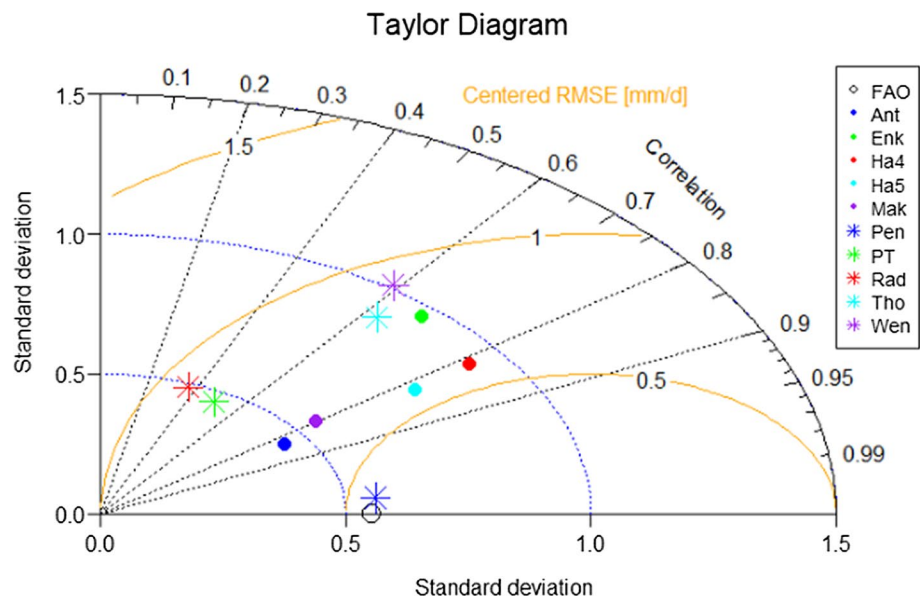


Mekoya (2020b) methods which require less data inputs, Eq. 2.2 and Eq. 2.5 can be used, respectively (see Table 2 and Table 3). The models can also be used for spatial mapping.

4.2 Conclusions

Generally, evapotranspiration (ET) has a crucial role in the land surface energy and hydrologic balances as well as in agricultural activities such as irrigation management in water stress areas. Because direct measurements are difficult, they are often replaced by indirect methods. Also, the lack of sufficient meteorological data is a constraint for estimating ET_0 from widely used well-known models such as the Food and Agricultural Organization method by Penman–Monteith (FAO56). Agricultural planning in arid and semi-arid areas cannot be achieved without an understanding of the meteorological parameters; particularly precipitation and evapotranspiration. While precipitation is measured, evapotranspiration can only be predicted from other climatic parameters. The approach is presumably simple but provides reliable estimates in the data-scarce conditions of Ethiopia. The methodology applied in this study can be extended and applied to any location in the world to understand the regional hydrological phenomena; for instance, to know the water resources capacity and the irrigation needs of East Africa.

Fig. 12 Taylor Diagram between FAO56 (FAO) and ten PET models at Nazareth (1982–2020)



The novelty of the study is that an old method by [42] (Wen) and a new method by [41] (Ant) which are applied for the first time in Ethiopia performed the best in estimating potential evapotranspiration (PET) over the study area without any calibration. Although these two methods had shown good performance in a few studies that they are applied, e.g., [26, 67], and [68], they have not often been used worldwide. For instance, PET by [41] was not even considered in the recent study which compared 127 PET models in two sites in Greece [26] that inturn makes this study unique.

4.3 Recommendations

In Ethiopia, particularly in Amhara and Oromia regional states where the five sites are located, if climate data is a constraint to compute ET_0 using the reference method (FAO56), ensembles of three or more of the best performed six PET models (Wen, Pen, Ant, PT, Mak, and Ha5) are recommended in Ethiopia because they can estimate ET_0 with reasonably good accuracy. However, to produce a more reliable result, a detailed investigation using long year (above 30 years) climate data from as many meteorological stations as possible (> 100 stations or > 300 grid points) that can represent the whole Ethiopia is recommended.

Acknowledgements The authors thank the Ethiopia Meteorology Institute (EMI) formerly called the National Meteorology Agency of Ethiopia (NMA) for providing the data used in this study. The authors also thank the Ethiopian Forestry development and the anonymous reviewers. Beloved parents and families and all who supported directly or indirectly for the success of this study are also acknowledged.

Author contributions Both authors contributed from concept development and research design to full writing up of the manuscript and have read and agreed publication.

Funding No funding has been received for the study.

Data availability The dataset used in this study can be found from third parties such as Ethiopia Meteorology Institute (<http://www.ethiomet.gov.et/>) and other climate dataset providers.

Declarations

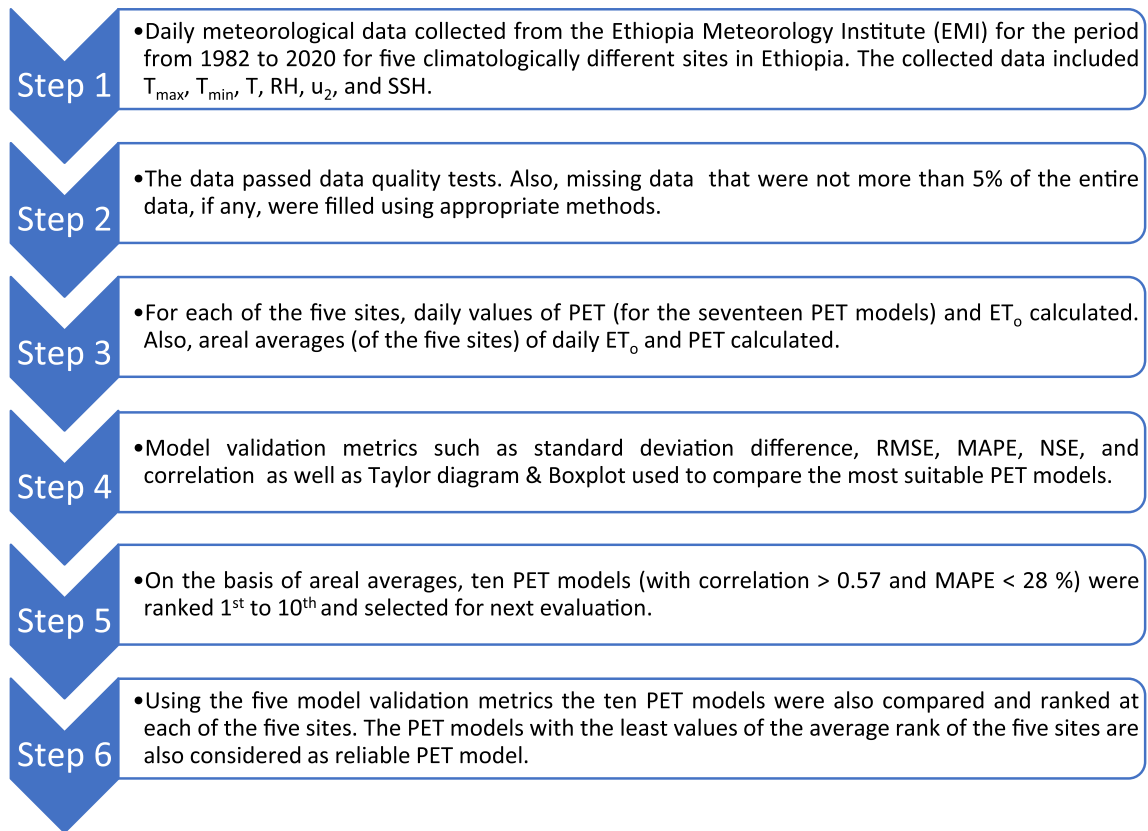
Ethical approval The manuscript has no ethical problem.

Competing interests The authors declare that they have no conflict of interest.

Open Access This article is licensed under a Creative Commons Attribution 4.0 International License, which permits use, sharing, adaptation, distribution and reproduction in any medium or format, as long as you give appropriate credit to the original author(s) and the source, provide a link to the Creative Commons licence, and indicate if changes were made. The images or other third party material in this article are included in the article's Creative Commons licence, unless indicated otherwise in a credit line to the material. If material is not included in the article's Creative Commons licence and your intended use is not permitted by statutory regulation or exceeds the permitted use, you will need to obtain permission directly from the copyright holder. To view a copy of this licence, visit <http://creativecommons.org/licenses/by/4.0/>.

Appendix 1

A scientific flowchart summarizing the comparison of seventeen PET models with ETo



References

1. M. Allen, Richard G, A, Luis S. 1998. RAES Dirk and SMITH. FAO Irrigation and drainage paper crop by. Irrig Drain. 300 56 300
2. Zeng Z, Peng L, Piao S. Response of terrestrial evapotranspiration to earth's greening. *Curr Opin Environ Sustain.* 2018;33:9–25. <https://doi.org/10.1016/j.cosust.2018.03.001>.
3. Paparrizos S, Matzarakis A. Present and future responses of growing degree days for crete Island in Greece. *Adv Sci Res.* 2017;14:1–5. <https://doi.org/10.5194/asr-14-1-2017>.
4. Irmak S, Irmak A, Howell TA, Martin DL, Payero JO, Copeland KS. Variability analyses of alfalfa-reference to grass-reference evapotranspiration ratios in growing and dormant seasons. *J Irrig Drain Eng.* 2008;134(2):147–59. [https://doi.org/10.1061/\(asce\)0733-9437\(2008\)134:2\(147\)](https://doi.org/10.1061/(asce)0733-9437(2008)134:2(147)).
5. Baumgartner A. The world water balance, mean annual global, continental and maritime precipitation, evaporation and runoff. *Agri Water Manage.* 1975;1(1):100–1.
6. Trenberth J, Kevine E, Fasullo J, Kiehl T. Earth's global energy budget. *Bull Am Meteorol Soc.* 2009;90(3):311–23. <https://doi.org/10.1175/2008BAMS2634.I>.

7. Yang Z, Zhang Q, Hao X. Evapotranspiration trend and its relationship with precipitation over the loess plateau during the last three decades. *Adv Meteorol.* 2016;2016:1–10.
8. Wang K, Dickinson RE. Estimating the total fertility rate from multiple imperfect data sources and assessing its uncertainty. *CRev Geophys.* 2012;50(RG2005):1–54. <https://doi.org/10.1029/2011RG000373.1>. INTRODUCTION.
9. Gao F, et al. Evaluation of reference evapotranspiration methods in arid, semiarid, and humid regions. *J Am Water Resour Assoc.* 2017;53(4):791–808. <https://doi.org/10.1111/1752-1688.12530>.
10. Jain SK, Nayak PC, Sudheer KP. Models for estimating evapotranspiration using artificial neural networks, and their physical interpretation. *Hydrol Process.* 2008;22(13):2225–34. <https://doi.org/10.1002/hyp.6819>.
11. Khoshravesh M, Sefidkouhi MAG, Valipour M. Estimation of reference evapotranspiration using multivariate fractional polynomial, Bayesian regression, and robust regression models in three arid environments. *Appl Water Sci.* 2017;7(4):1911–22. <https://doi.org/10.1007/s13201-015-0368-x>.
12. Ding R, Kang S, Li F, Zhang Y, Tong L. Evapotranspiration measurement and estimation using modified Priestley-Taylor model in an irrigated maize field with mulching. *Agric For Meteorol.* 2013;168:140–8. <https://doi.org/10.1016/j.agrformet.2012.08.003>.
13. McMahon TA, Peel MC, Lowe L, Srikanthan R, McVicar TR. Estimating actual, potential, reference crop and pan evaporation using standard meteorological data: a pragmatic synthesis. *Hydrol Earth Syst Sci.* 2013;17(4):1331–63. <https://doi.org/10.5194/hess-17-1331-2013>.
14. Xiang K, Li Y, Horton R, Feng H. Similarity and difference of potential evapotranspiration and reference crop evapotranspiration—a review. *Agric Water Manag.* 2019;232(August):2020. <https://doi.org/10.1016/j.agwat.2020.106043>.
15. Dingman SL. *PHYSICAL Third Edition.* 1992.
16. Li S, et al. Evaluation of six potential evapotranspiration models for estimating crop potential and actual evapotranspiration in arid regions. *J Hydrol.* 2016;543:450–61. <https://doi.org/10.1016/j.jhydrol.2016.10.022>.
17. Monteith P. A Comparative study of potential evapotranspiration estimation by eight methods with FAO. *Water.* 2017. <https://doi.org/10.3390/w9100734>.
18. Peng L, Li Y, Feng H. The best alternative for estimating reference crop evapotranspiration in different sub-regions of mainland China. *Sci Rep.* 2017;7(1):1–19. <https://doi.org/10.1038/s41598-017-05660-y>.
19. Enku T, Van Der Tol C, Gieske A, Rientjes T. Evapotranspiration modeling using remote sensing and empirical models in metadata of the chapter that will be visualized online. *Nile River Basin Hydrol Clim Water Use.* 2011. <https://doi.org/10.1007/978-94-007-0689-7>.
20. Xie R, Wang A. Comparison of ten potential evapotranspiration models and their attribution analyses for ten Chinese drainage Basins. *Adv Atmos Sci.* 2020;37(9):959–74. <https://doi.org/10.1007/s00376-020-2105-0>.
21. Jacobs JM, Anderson MC, Friess LC, Diak GR. Solar radiation, longwave radiation and emergent wetland evapotranspiration estimates from satellite data in Florida, USA. *Hydrol Sci J.* 2004;49(3):461–76. <https://doi.org/10.1623/hysj.49.3.461.54352>.
22. Lu J, Sun G, McNulty SG, Amatya DM. A comparison of six potential evapotranspiration methods for regional use in the southeastern United States. *J Am Water Resour Assoc.* 2005;41(3):621–33. <https://doi.org/10.1111/j.1752-1688.2005.tb03759.x>.
23. Douglas EM, Jacobs JM, Sumner DM, Ray RL. A comparison of models for estimating potential evapotranspiration for Florida land cover types. *J Hydrol.* 2009;373(3–4):366–76. <https://doi.org/10.1016/j.jhydrol.2009.04.029>.
24. Donohue RJ, McVicar TR, Roderick ML. Assessing the ability of potential evaporation formulations to capture the dynamics in evaporative demand within a changing climate. *J Hydrol.* 2010;386(1–4):186–97. <https://doi.org/10.1016/j.jhydrol.2010.03.020>.
25. Bormann H. Sensitivity analysis of 18 different potential evapotranspiration models to observed climatic change at German climate stations. *Clim Change.* 2011;104(3–4):729–53. <https://doi.org/10.1007/s10584-010-9869-7>.
26. Proutsos N, et al. A thorough evaluation of 127 potential evapotranspiration models in two mediterranean Urban Green Sites. *Remote Sens.* 2023;15(14):1–41. <https://doi.org/10.3390/rs15143680>.
27. Xu CY, Singh VP. Evaluation and generalization of temperature-based methods for calculating evaporation. *Hydrol Process.* 2001;15(2):305–19. <https://doi.org/10.1002/hyp.119>.
28. Seleshi Y. Calibration of the priestley-taylor evaporation model for Ethiopia. *Zede J.* 2018;36:28–40.
29. Enku AM. Temesgen; melesse a simple temperature method for the estimation of evapotranspiration". *Hydrol Process Hydrol Process.* 2013. <https://doi.org/10.1002/hyp.9844>.
30. Adem AA, Aynalem DW, Tilahun SA, Steenhuis TS. Predicting reference evaporation for the Ethiopian highlands. *J Water Resour Prot.* 2017;09(11):1244–69. <https://doi.org/10.4236/jwarp.2017.911081>.
31. Belete MD, Diekkrüger B, Roehrig J. Linkage between water level dynamics and climate variability: The case of lake hawassa hydrology and ENSO Phenomena. *Climate.* 2017;5(1):21. <https://doi.org/10.3390/cli5010021>.
32. Nyssen J, et al. Rainfall erosivity and variability in the Northern Ethiopian Highlands. *J Hydrol.* 2005;311(1–4):172–87. <https://doi.org/10.1016/j.jhydrol.2004.12.016>.
33. Hurni H. Degradation and conservation of the resources in the Ethiopian highlands. *Mt Res Dev.* 1988;8(2–3):123–30. <https://doi.org/10.2307/3673438>.
34. Legese W, Koricha D, Ture K. Characteristics of seasonal rainfall and its distribution over bale highland, southeastern Ethiopia. *J Earth Sci Clim Change.* 2018. <https://doi.org/10.4172/2157-7617.1000443>.
35. Ayalew D. Variability of rainfall and its current trend in Amhara region, Ethiopia. *African J Agric Res.* 2012. <https://doi.org/10.5897/ajar11.698>.
36. Mekuyie M, Mulu D. Perception of impacts of climate variability on pastoralists and their adaptation/coping strategies in fentale district of oromia region, Ethiopia. *Environ Syst Res.* 2021. <https://doi.org/10.1186/s40068-020-00212-2>.
37. Snyder S. The ASCE standardized reference evapotranspiration equation appendices A-F draft toxicol relev EDCs pharm. *Drink Water.* 2002
38. Melesse AM, Abteu W, Dessalegne T. Evaporation estimation of Rift Valley lakes: comparison of models. *Sensors.* 2009;9(12):9603–15. <https://doi.org/10.3390/s91209603>.
39. Aschonitis VG, Antonopoulos VZ, Papamichail DM. Evaluation of pan coefficient equations in a semi-arid Mediterranean environment using the ASCE-standardized Penman-Monteith method. *Agric Sci.* 2012;03(01):58–65. <https://doi.org/10.4236/as.2012.31008>.
40. W. M. O. WMO and U. N. E. and S. O. UNESCO. *International Glossary of Hydrology.* 12. 1998
41. Mekoya A. Dependency of evaporation and class a pan coefficient on meteorological parameters. *Int J Environ Sci Nat Resour.* 2020. <https://doi.org/10.19080/ijesnr.2020.24.556134>.

42. Wendling U. Schätzmethode der Verdunstung landwirtschaftlicher Bestände nach den Ansätzen von Penman und Turc. = 'estimating evaporation in crop stands according to Penman and Turc formulas'. (in German, with English summary). *Arch AckerPflanzenbau Bodenkd.* 1991;35(35):251–7.
43. Mekoya A. Evaluation of evaporation paradox at tharandt. *Int J Environ Sci Nat Resour.* 2020. <https://doi.org/10.19080/ijesnr.2020.24.556142>.
44. Goh EH, Ng JL, Huang YF, Yong SLS. Performance of potential evapotranspiration models in Peninsular Malaysia. *J Water Clim Chang.* 2021;12(7):3170–86. <https://doi.org/10.2166/wcc.2021.018>.
45. Bakhtiari B, Ghahreman N, Liaghat AM, Hoogenboom G. Evaluation of reference evapotranspiration models for a semiarid environment using lysimeter measurements. *J Agric Sci Technol.* 2011;13(2):223–37.
46. Djaman K, et al. Evaluation of sixteen reference evapotranspiration methods under sahelian conditions in the Senegal River Valley. *J Hydrol Reg Stud.* 2015;3:139–59. <https://doi.org/10.1016/j.ejrh.2015.02.002>.
47. Tukimat NNA, Harun S, Shahid S. Comparison of different methods in estimating potential évapotranspiration at Muda Irrigation Scheme of Malaysia. *J Agric Rural Dev Trop Subtrop.* 2012;113(1):77–85.
48. Hargreaves GH, Samani ZA. Reference crop evapotranspiration from ambient air temperature. *Pap Am Soc Agric Eng.* 1985. <https://doi.org/10.13031/2013.26773>.
49. Oudin L, et al. Which potential evapotranspiration input for a lumped rainfall-runoff model? Part 2 - Towards a simple and efficient potential evapotranspiration model for rainfall-runoff modelling. *J Hydrol.* 2005;303(1–4):290–306. <https://doi.org/10.1016/j.jhydrol.2004.08.026>.
50. Chang X, Wang S, Gao Z, Luo Y, Chen H. Forecast of daily reference evapotranspiration using a modified daily thornthwaite equation and temperature forecasts. *Irrig Drain.* 2019;68(2):297–317. <https://doi.org/10.1002/ird.2309>.
51. Sharafi S, Mohammadi Ghalemi M. Calibration of empirical equations for estimating reference evapotranspiration in different climates of Iran. *Theor Appl Climatol.* 2021;145(3):925–39. <https://doi.org/10.1007/s00704-021-03654-5>.
52. Ndulue E, Onyekwelu I, Ogbu KN, Ogwo V. Performance evaluation of solar radiation equations for estimating reference evapotranspiration (ET₀) in a humid tropical environment. *J Water L Dev.* 2019;42(1):124–35. <https://doi.org/10.2478/jwld-2019-0053>.
53. Dubovský V, Dlouhá D, Pospíšil L. The calibration of evaporation models against the penman-monteith equation on lake most. *Sustain.* 2021;13(1):1–17. <https://doi.org/10.3390/su13010313>.
54. Mahmud K, Siddik M, Khatun M, Islam M. Performance evaluation of Class A pan coefficient models to estimate reference evapotranspiration in Mymensingh region of Bangladesh. *J Bangladesh Agric Univ.* 2020. <https://doi.org/10.5455/jbau.101511>.
55. Melišová E, Vizina A, Hanel M, Pavlík P, Šuhájková P. Evaluation of evaporation from water reservoirs in local conditions at czech republic. *Hydrology.* 2021;8(4):1–17. <https://doi.org/10.3390/hydrology8040153>.
56. Ferreira RC, Abi-Saab OJG. Evaluation of alternative methods to calculate evapotranspiration and their impact on soybean yield estimation. *Agrometeoros.* 2020. <https://doi.org/10.31062/agrom.v28.e026753>.
57. Sriram AV, Rashmi C. Estimation of potential evapotranspiration by multiple linear regression method. *IOSR J Mech Civ Eng.* 2014;11(2):65–70. <https://doi.org/10.9790/1684-11246570>.
58. Irmak S, Haman DZ, Jones JW. Evaluation of class A pan coefficients for estimating reference evapotranspiration in humid location. *J Irrig Drain Eng.* 2002;128(3):153–9. [https://doi.org/10.1061/\(asce\)0733-9437\(2002\)128:3\(153\)](https://doi.org/10.1061/(asce)0733-9437(2002)128:3(153)).
59. Legates DR, McCabe GJ. Evaluating the use of 'goodness-of-fit' measures in hydrologic and hydroclimatic model validation. *Water Resour Res.* 1999;35(1):233–41. <https://doi.org/10.1029/1998WR900018>.
60. Krause P, Boyle DP, Bäse F. 2014 "Comparison of different efficiency criteria for hydrological model assessment." *Adv Geosci.* 2005;5:89–97. <https://doi.org/10.5194/adgeo-5-89-2005>.
61. Khairy WM, El-Motasem M, Mehanna A, Hefny K. Estimation of evaporation losses from water bodies in the Sudan and Ethiopia. *Int J Energy Water Resour.* 2019;3(3):233–46. <https://doi.org/10.1007/s42108-019-00031-x>.
62. "Muhammad et al., 2019 Evaluation of Empirical Reference Evapotranspiration Models Using Compromise Programming A Case Study of Peninsular Malaysia.pdf"
63. A. Gorjizade, A. Akhondali, H. Zarei, H. S. Kaboli, I. J. Adv, and B. Biom. Evaluation of Eight evaporation estimation methods in a semi-arid region (Dez reservoir , Iran) 2 5: 1823–1836. 2014.
64. Dechasa S, Koteswararao B, Unduche FS. Biophysical characteristics of weyb watershed, bale mountainous area of the Southeastern Ethiopia. *Management.* 2019;9:515–21. <https://doi.org/10.3540/ijitee.17725.078919>.
65. Ayenew T. Evapotranspiration estimation using thematic mapper spectral satellite data in the Ethiopian rift and adjacent highlands. *J Hydrol.* 2003;279(1–4):83–93. [https://doi.org/10.1016/S0022-1694\(03\)00173-2](https://doi.org/10.1016/S0022-1694(03)00173-2).
66. "Ashemi. Estimation of reference evapotranspiration by using different five empirical models for Melkassa Area, Central Rift Valley of Ethiopia. pdf. 2021.
67. Mekoya A. Comparison of evaporation schemes and methods of estimation of class a pan coefficient at tharandt, Germany. *Water Conserv Sci Eng.* 2021;6(1):25–35. <https://doi.org/10.1007/s41101-020-00099-1>.
68. Mekoya A. Estimation of evaporation at tharandt, using daily and ten-minute class-a pan data from automatic measuring pressure sensor instrument. *J Environ Sci Nat Resour Int.* 2019. <https://doi.org/10.1908/ijesnr.2019.19.556003>.

Publisher's Note Springer Nature remains neutral with regard to jurisdictional claims in published maps and institutional affiliations.